Journal of Organometallic Chemistry, 467 (1994) 135–143

Substituted cyclopentadienyl compounds

III *. NMR and molecular orbital study of conformational preferences in some substituted (η^5-cyclopentadienyl)-rhodium(η^4-diene) compounds and the crystal structure of (η^5-methanoylcyclopentadienyl)-(η^4-2,3-dimethoxybutadiene)rhodium(I)

Michael Arthurs, John Bickerton, Gina Kubal, Julie O'Sullivan and Colin Piper
Division of Chemistry, School of Natural and Environmental Sciences, Coventry University, Priory Street, Coventry CV1 5FB (UK)

Graeme Hogarth
Chemistry Department, Christopher Ingold Laboratories, University College London, 20 Gordon Street, London WC1 0AJ (UK)

D. Antony Morton-Blake
Department of Chemistry, University of Dublin, Trinity College, Dublin 2 (Ireland)

(Received April 5, 1993)

Abstract

The crystal structure of (η^5-C_5H_4CHO)Rh(η^4-$C_4H_4(OMe)_2$) (I) has been determined by X-ray diffraction. The preferred orientation of the ligands is one in which the cyclopentadienyl ring substituent bond bisects the internal carbon–carbon bond of the counter diene ligand. Related compounds for which four separate ring resonances appear have been analysed by nOe difference NMR spectroscopy and spectral simulation. The results show that the preferred relative orientation of ligands in solution is similar to that revealed by crystallographic studies. CNDO/U molecular orbital calculations have been performed on several of these compounds. The results are consistent with experimental findings and show that there is a preference for a rotamer in which the ring has a tendency towards the allyl-ene geometry. Carbon-13 NMR studies show that the ratios of the diene carbon chemical shifts and metal–diene coupling constants reflect the relative importance of retrodative bonding.

Key words: Rhodium; Cyclopentadienyl; π-Bonding; Nuclear magnetic resonance; Molecular orbital calculations; Crystal structure

1. Introduction

Since the discovery [2] that ligand displacement in η^5-$C_5H_5Rh(CO)_2$ complexes by phosphine or phosphite involves an S_N2 pathway, there has been considerable progress in this area of chemistry. Cheong and Basolo [3] found that carbonyl substitution in η^5-$C_5H_4XRh(CO)_2$ is facilitated when X is electron accepting, and the transition state or intermediate in such reactions has been shown to possess an η^3-allyl-ene ring structure [4]. Techniques such as ^{59}Co NMR spectroscopy [5], photoelectron spectroscopy [6], core and valence ionization studies [4] and Hückel molecular orbital calculations [7] have been employed in the assessment of slippage and catalytic potential of related η^5-$C_5H_4XCoL_2$ (L = CO or C_2H_4) complexes. Our initial ^{1}H NMR analysis of analogous rhodium systems showed that cp ring slippage is less pronounced for bis(carbonyl) than for bis(ethene)-rhodium compounds in the ground state [8]. However, it is clear

---

Correspondence to: Dr. M. Arthurs.

* For Part II, see ref. 1.

0022-328X/94/$7.00
SSDI 0022-328X(93)23990-F

© 1994 – Elsevier Sequoia. All rights reserved

that S_N2 substitution reactions involving the former systems [3] occur more easily than those involving bis(ethene) analogues [9]. This may be associated with a smaller activation energy for the η^5- to η^3-allyl reorganization. The importance of ring slippage in substitution reactions involving η^5-C_5H_4XCo (COD) complexes is less clear since both S_N1 and S_N2 pathways have been identified [6]. The latter does however, become dominant when X is strongly electron accepting. Clearly there is need to examine the relationship between structure and bonding on the one hand and reactivity on the other hand for these Group 9 metal systems. As part of our current interest in the former, we recently noted [1] that the preferred orientation of ligands and nature of the associated slippage in the solid state in η^5-$C_5H_4XRh(C_2H_4)_2$ systems are profoundly affected by the way in which X interacts with the Cp ring. Herein we report on the conformational preferences observed for (η^4-1,3-diene)Rh(η^5-C_5H_4X) compounds in solution and the solid state. NMR and CNDO/U molecular orbital data are presented for several of these compounds.

2. Experimental details

Most of the NMR spectra were recorded on a Bruker AC-250 spectrometer fitted with variable-temperature accessories; the probe temperature was calibrated by van Geet's method [10]. NOE difference spectra were recorded on a Bruker WH-400 spectrometer at the S.E.R.C. high field NMR service, University of Warwick. The simulation study of the cp signals in the ^1H NMR spectra of **VI** and **VII** was obtained with Gaussian enhancement by use of the PANIC (parameter adjustment in NMR by iterative calculation) program. Elemental analyses were performed by C.H.N. Analysis Ltd., Leicester, and Butterworth Laboratories Ltd., Teddington, Middx. Mass spectra were recorded on Kratos MS-80 and AEI MS-30 instruments. IR spectra were recorded over the range 4000–250 cm^{-1} on a Perkin–Elmer 577 spectrophotometer. Melting points were determined on a Kofler micro hot-stage apparatus. All reactions were carried out under nitrogen in dry degassed solvents. Dienes were purchased from Aldrich Chemicals and used without further purification. Rhodium compounds were prepared by the methods described previously for **III–VII** [11]. The synthesis of **I** is typical: 778 mg (2 mmol) of $[(C_2H_4)_2RhCl]_2$ was suspended in diethyl ether (50 cm^3). An excess (684 mg, 6 mmol) of 2,3-dimethoxybutadiene was added and the mixture stirred vigorously for 30 min. The yellow chloro-bridged intermediate was filtered off and washed with pentane. Treatment of this solid with a stoichiometric equivalent of potassium methanoylcyclopentadienide in ether followed by filtration, evaporation of the filtrate and recrystallization of the residue from hexane gave **I** with a 65% yield, m.p., 77–78°C. Anal. Found: C, 46.35; H, 5.08. $C_{12}H_{15}O_3Rh$ calc.: C, 46.45; H, 4.84%. MS: m/e 310 (M^+). Similarly, **II** was isolated with a 60% yield as a yellow solid (m.p., 97–98°C). Anal. Found: C, 46.94; H, 5.53. $C_{11}H_{15}O_2Rh$ calc.: C, 46.81; H, 5.32%. MS: m/e 282 (M^+).

2.1. Crystal structure determination for I

The crystal data for $[C_5H_4CHO]Rh[C_4H_4(OMe)_2]$ are as follows: $C_{12}H_{15}O_3Rh$; $M = 310.2$; orthorhombic; $a = 10.383(6)$ Å, $b = 14.018(6)$ Å and $c = 16.630(9)$ Å; $U = 2420.63$ Å^3; $D_c = 1.700$ g cm^{-3}; $Z = 8$; F(000) = 1248; space group, *PbCa*; μ(Mo Kα) = 1.38 cm^{-1}; $\lambda = 0.717073$ Å.

A suitable crystal was obtained by slow recrystallization from hexane at 5°C. A yellow crystal of approximate dimensions 0.40 × 0.28 × 0.16 mm was mounted on a glass fibre. All geometric and intensity data were taken from this sample using an automated Nicolet R3mV four-circle diffractometer. The lattice vectors were identified by application of the automatic indexing routine of the diffractometer to the positions of 25 reflections taken from a rotation photograph and centred by the diffractometer. The ω–2θ scan technique was used to measure 2388 reflections, of which 2097 were unique in the range $2° \leqslant 2\theta \leqslant 50°$. Three intensity standards were measured every 97 reflections and showed no significant loss of intensity. Data were corrected for Lorentz and polarization effects, and empirically for absorption. Processing of the measured data gave 1544 reflections with $I \geqslant 3.0\sigma(I)$, and these were used to solve and refine the structure in the orthorhombic space group *Pbca*. The structure was solved by direct methods and developed by using alternating cycles of least-squares refinement and difference Fourier synthesis. The non-hydrogen atoms were refined anisotropically while hydrogen atoms were placed in calculated positions and assigned a common isotropic thermal parameter ($U = 0.08$ Å^2). The structure was given a weighting scheme of the form $\omega = 1/[\sigma^2(F) + 0.001878F^2]$. The final cycle of least-squares refinement included 145 parameters for 1544 observations and did not show shifts for any parameter of more than 0.002 times the standard deviation. Refinement converged with $R = 0.072$ and $R_w = 0.073$, and the final difference Fourier was featureless with no peaks greater than 0.91 eÅ^{-3}. Calculations were carried out with the SHELXTL PLUS program on the Microvax II computer at University College, London. Atomic coordinates are given in Table 1, selected bond lengths and angles in Table 2, and least-squares planes in Table 3. Tables of anisotropic thermal parameters, H atom co-

TABLE 1. Atomic coordinates ($\times 10^4$) and equivalent isotropic displacement parameters ($Å^2 \times 10^3$) for (η^5-C_5H_4CHO)Rh(η^4-$C_4H_4(OMe)_2$)

Atom	x	y	z	U_{eq} [a]
Rh	823(1)	970(1)	1348(1)	34(1)
O(1)	−2822(10)	1705(8)	811(8)	90(5)
O(2)	2414(8)	−443(6)	2383(4)	48(3)
O(3)	3679(8)	283(7)	1163(5)	51(3)
C(1)	483(11)	2458(9)	992(9)	53(4)
C(2)	1258(15)	2502(10)	1687(11)	68(5)
C(3)	580(15)	2088(10)	2323(8)	63(5)
C(4)	−623(14)	1176(9)	2036(8)	57(5)
C(5)	−707(12)	2045(9)	1206(7)	52(4)
C(6)	−1792(12)	1922(9)	651(9)	59(5)
C(7)	383(11)	−493(9)	1598(8)	45(4)
C(8)	1738(11)	−327(7)	1708(7)	37(3)
C(9)	2414(11)	78(9)	1041(6)	42(3)
C(10)	1676(13)	294(10)	337(7)	55(5)
C(11)	1769(15)	−573(11)	3114(8)	67(5)
C(12)	4243(15)	988(14)	652(11)	107(9)

[a] U_{eq} is defined as one third of the trace of the orthogonalized U_{ij} tensor.

TABLE 2. Selected bond lengths (pm) and angles (°) for [(η^5-C_5H_4CHO)Rh(η^4-$C_4H_4(OMe)_2$)]

Bond lengths			
Rh–C(1)	219.7(13)	Rh–C(2)	226.6(14)
Rh–C(3)	226.8(14)	Rh–C(4)	219.9(13)
Rh–C(5)	220.2(12)	Rh–C(7)	214.2(12)
Rh–C(8)	213.7(10)	Rh–C(9)	213.5(12)
Rh–C(10)	212.3(13)		
C(1)–C(2)	140.9(22)	C(2)–C(3)	139.6(22)
C(3)–C(4)	140.6(20)	C(4)–C(5)	143.4(18)
C(5)–C(1)	140.9(17)	C(5)–C(6)	146.7(18)
C(6)–O(1)	114.4(16)	C(7)–C(8)	143.8(16)
C(8)–C(9)	143.0(16)	C(9)–C(10)	143.1(16)
C(8)–O(2)	133.5(14)	C(9)–O(3)	136.0(14)
Bond angles			
C(1)–C(2)–C(3)	108.3(13)	C(2)–C(3)–C(4)	108.7(13)
C(3)–C(4)–C(5)	107.3(11)	C(4)–C(5)–C(1)	107.3(11)
C(5)–C(1)–C(2)	108.2(12)	C(5)–C(6)–O(1)	124.2(12)
C(7)–C(8)–C(9)	116.5(10)	C(8)–C(9)–C(10)	117.1(10)

TABLE 3. Least-squares planes

Distances (pm) of atoms from plane 1	C(1), −2; C(2), 1; C(3), 1; C(4), −2; C(5), 2; C(6), 7; Rh [a], −187
Distances (pm) of atoms from plane 2	C(7), −0; C(8), 1; C(9), −1; C(10), 0; Rh [a], 164
Angle between planes	12.9°

[a] Atoms not contributing to the planes.

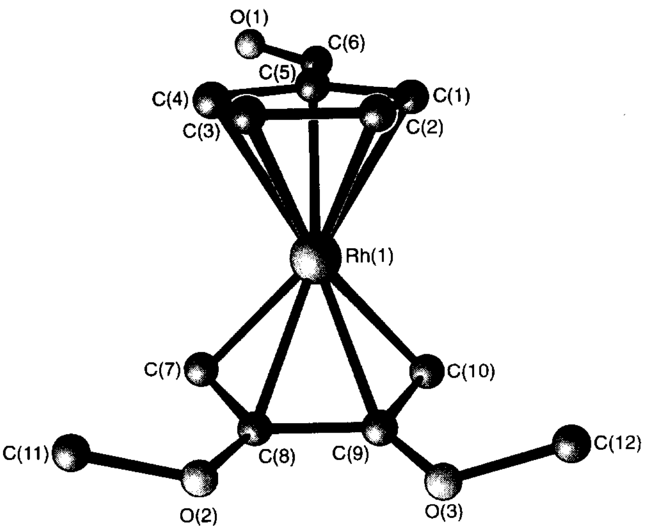

Fig. 1. The molecular structure of [(η^5-C_5H_4CHO)Rh(η^4-$C_4H_4(OMe)_2$] (I) with the atom labelling.

ordinates, and the complete list of molecular dimensions have been deposited with the Cambridge Crystallographic Data Centre.

3. Discussion

3.1. Structure and bonding considerations

The structure of I is shown in Fig. 1. There are no intermolecular contacts less than the sum of the van der Waals radii. The 1,3-diene is oriented such that the C(7)–C(8) and C(9)–C(10) bonds are approximately parallel to the C(3)–C(4) and C(1)–C(2) ring bonds. The values of the least-squares planes (Table 3) provide some evidence for a slight ring puckering, with C(1) and C(4) deviating from the mean plane by 2 pm towards the rhodium atom, and C(2), C(3) and C(5) deviating by 1 pm, 1 pm and 2 pm respectively away from the rhodium. The aldehydic carbon C(6) is also displaced by 7 pm away from the rhodium. Although the r.m.s. deviation of the five ring carbon atoms is only 1.45 pm, the pattern of the individual deviations mirrors that observed by Lichtenberger *et al.* [12], for η^5-$C_5Me_5Rh(CO)_2$, in which a significant bonding distortion of the allyl-ene type is present. In I a similar tendency is shown by the differences between Rh–C bond distances to the Cp ring. The shortest bonds are to C(1) (219.7(13) pm), C(4) (219.9(13) pm) and C(5) (220.2(12) pm), while the longest bonds are those from the metal to C(2) (226.6(14) pm) and C(3) (226.8(14) pm). The short C(5)–C(6) distance of 146.7(18) pm implies the presence of some delocalization over ring and substituent, as previously noted for η^5-C_5H_4CO-OMeRh(1,5-COD) [8]. There are no significant variations in the carbon–carbon or rhodium–carbon dis-

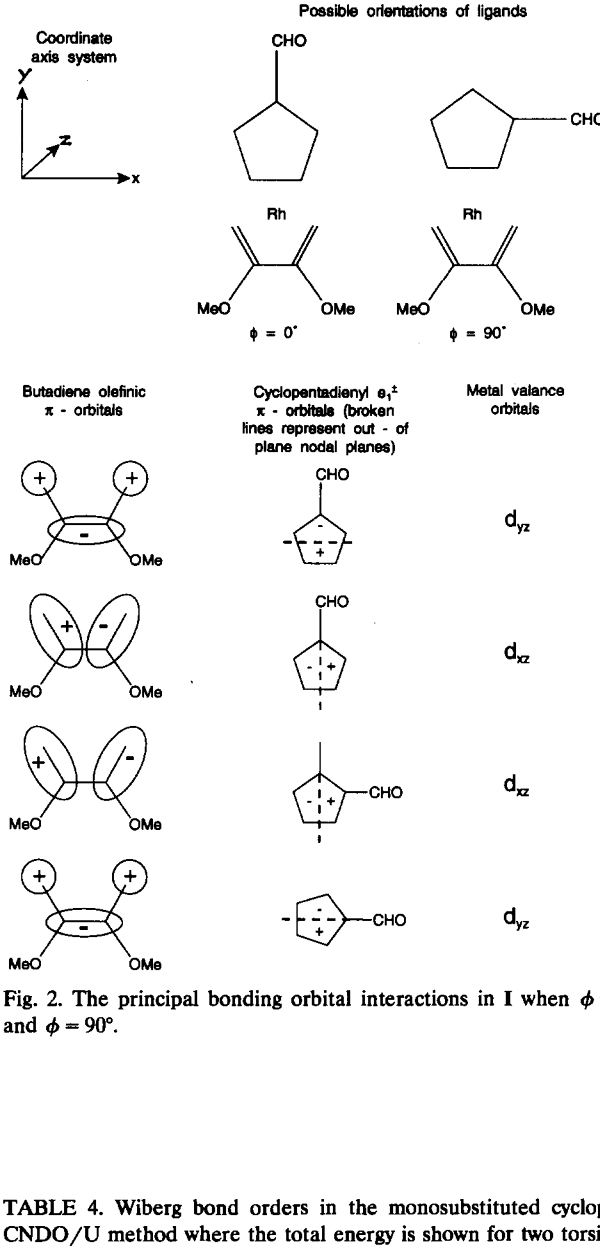

Fig. 2. The principal bonding orbital interactions in I when $\phi = 0°$ and $\phi = 90°$.

tances relating to the butadiene ligand in I. The average rhodium–diene carbon distance (C(7), C(8), C(9) and C(10)) is 213.4(13) pm, a value comparable with that found for $(\eta^5\text{-}C_5H_5)Rh(\eta^4\text{-}2,3\text{-dichlorobutadiene})$, in which the corresponding average is 212.9(16) pm [13], although it is noteworthy that the inner carbon atoms of the diene ligand are marginally closer to rhodium (209.1(14) pm) than the terminal carbon atoms (213.0(15) pm) in the latter case. This difference in metal–diene bonding probably originates from the differing π acceptor characteristics of the competing Cp and diene ligands in the two complexes. The origins of the allyl-ene bonding mode in I derive from the nodal characteristics of the HOMO in the Cp e_1 set. Figure 2 shows the principal interacting ligand orbitals under the designated coordinate system and defines two possible torsional orientations of the ligand systems as $\phi = 0°$ and $\phi = 90°$, in accord with our previous molecular orbital discussion of ring–metal bonding in $\eta^5\text{-}C_5H_4XRh\ (C_2H_4)_2$ compounds [1]. The solid state structure of I is thus in accord with an orientation defined by $\phi = 0°$. Hence the principal bonding interactions involve the ring e_1^+ and diene Ψ_2 molecular orbitals interacting with the empty metal d_{xz} hybrid and the diene Ψ_3 and ring e_1^- molecular orbitals interacting with the filled d_{yz} hybrid. The latter interaction gives rise to the HOMO in the complex, and the observed distortion derives from the greater importance of diene-yl like bonding to create a ring with some allyl-ene structure. Conversely, if the cp ring is rotated by 90° in the xz plane ($\phi = 90°$) the allyl-ene bonding becomes more important and a ring with some diene-yl structure is created. In order to compare the

TABLE 4. Wiberg bond orders in the monosubstituted cyclopentadienyl ring in $[(\text{olefin})Rh(\eta^5\text{-}C_5H_4X)]$ compounds as calculated by the CNDO/U method where the total energy is shown for two torsional orientations of the olefin and cp ring

Olefin	x	ϕ (°)	p_{51}	p_{12}	p_{23}	p_{34}	p_{45}	Energy (eV)
—	Rh–Cp	–	1.3221	1.3221	1.3221	1.3221	1.3221	–
$(C_2H_4)_2$	H	0	1.3281	1.1704	1.4395	1.1704	1.3281	−2599.4541
		90	1.2374	1.4072	1.1465	1.4071	1.2374	−2599.4541
$C_4H_4(OMe)_2$ [a]	CHO	0	1.2894	1.1515	1.5285	1.1520	1.2836	−4744.6621
		90	1.1812	1.5166	1.0952	1.5016	1.1688	−4744.5000
$C_4H_4(C_6H_5)_2$ [b]	CHO	0	1.2858	1.1644	1.5079	1.1643	1.2812	−5665.8125
		90	1.1867	1.5066	1.1062	1.4903	1.1747	−5665.5898
$(C_2H_4)_2$	CHO	0	1.2745	1.1947	1.4212	1.1933	1.2734	−3289.8809
		90	1.2026	1.4188	1.1451	1.4174	1.2057	−3289.7686

[a] 2,3-Dimethoxybutadiene
[b] *trans,trans*-1,4-Diphenylbutadiene.

TABLE 5. Hydrogen-1 nuclear magnetic resonance spectral data for $[(\eta^5\text{-}C_5H_4X)Rh(diolefin)$ with ^{103}Rh coupling constants in parentheses [a]

Compound	Diolefin	X	^1H NMR, δ [b] (ppm)										
			H(1)	H(4)	H(2)	H(3)	X	H(7_a)	H(10_a)	H(7_s)	H(10_s)	H(8)	H(9)
I	2,3-Dimethoxy-butadiene	CHO	5.92 (td, J = 0.8 Hz)		5.38 (tq, J = 0.9 Hz)		9.71 (s)	0.09 (dd, J = 2.8 Hz)		2.74 (dd, J = 0.9 Hz)		3.44 (s, Me)	
II	2,3-Dimethoxy-butadiene	H	5.32 (d, J = 0.9 Hz)					−0.27 (dd, J = 2.6 Hz)		2.58 (dd, J = 0.9 Hz)		3.44 (s, Me)	
III	*trans,trans*-1,4-Diphenylbutadiene	CHO	4.65 (td, J = 0.5 Hz)		5.14 (tq, J = 0.9 Hz)		9.56 (s)	2.62 (dd, J = 2.2 Hz)		7.20 (m, Ph)		5.53 (dd, J = 1.5 Hz)	
IV	*trans,trans*-1,4-Diphenylbutadiene	COOMe	4.99 (td, J = 0.8 Hz)		4.90 (td, J = 1.0 Hz)		3.50 (s)	2.46 (dd, J = 2.2 Hz)		7.19 (m, Ph)		5.46 (dd, J = 1.5 Hz)	
V	2,3-Dimethyl-butadiene	CHO	5.67 (td, J = 0.7 Hz)		5.38 (tq, J = 0.9 Hz)		9.58 (s)	0.49 (t, J = 1.9 Hz)		2.57 (t, J = 0.4 Hz)		2.05 (s, Me)	
VI	*cis*-3-Methyl-pentadiene	COOMe	5.65 (m, J = 0.7 Hz)	5.83 (m, J = 0.8 Hz)	5.24 (m, J = 0.9 Hz)	5.44 (m, J = 0.9 Hz)	3.66 (s)	1.40 (tt), J = 2.4 Hz)	0.90 (d, J = 0.8 Hz)	2.45 (qq, J = 0.9 Hz)	3.40 (m, J = 1.2 Hz)	4.96 (m, J = 1.4 Hz)	1.90 (s, Me)
VII	2-methyl-1,4-pentadiene [c]	COOMe	5.29 (m, J = 0.5 Hz) [5.17] [d]	5.37 (m, J = 0.5 Hz) [5.26] [d]	5.21 (m, J = 0.9 Hz) [5.22] [d]	5.42 (m, J = 0.9 Hz) [5.49] [d]	3.78 (s)	1.24 (d)	1.32 (dd)	2.32 (t)	2.44 (tt)	1.63 (s, Me)	3.35 (m)

[a] Values in square brackets recorded in $CDCl_3$ at 294 K relative to internal $SiMe_4$.

[b] s, singlet; d, doublet; t, triplet; q, quartet; dd, doublet of doublets; tt, triplet of triplets; tq, triplet of quartets; qq, quartet of quartets; m, multiplet.

[c] Rhodium-1,4-diene coupling is less than 0.4 Hz; chemical shifts of central *exo* and *endo* diene hydrogen nuclei are δ 2.67 ppm (H_{exo}) and 2.23 ppm (H_{endo}).

[d] Chemical shifts at 213 K.

relative stabilities of these two torsional isomers the total molecular energy and Wiberg bond orders were calculated by CNDO/U [14], and the results are presented in Table 4. The variation in bond order in each case is that expected for a population of conformers in which the allyl-ene form is more highly populated when $\phi = 0°$ and the diene-yl form more populated when $\phi = 90°$. When the ring is unsubstituted, there is no electronic preference, and these two types of conformers are equienergetic. However, when a methanoyl substituent is present in the Cp ring, the favoured rotamer is always allyl-ene. The reason for this preference was discussed previously [1] and is associated with the mechanism by which the substituent interacts with the π molecular orbitals of the Cp ring. In view of the fact that the diene in **I** is a better π acceptor [15] than ethene, we had hoped to find some difference in the preference for the allyl-ene rotamer. Table 4 shows, however, that the energy difference between diene-yl and allyl-ene rotamers is largest for the *trans,trans*-1,4-diphenylbutadiene compound (**III**). A partial explanation for this difference between **I** and **III** can be found in the relatively higher energy associated with the diene Ψ_3 LUMO in **III** [16]. In view of the possible contribution of crystal packing requirements or crystallographically imposed symmetry constraints to the appropriate localized geometry we decided to investigate the conformational behaviour of some analogous compounds in solution, and the results are discussed below.

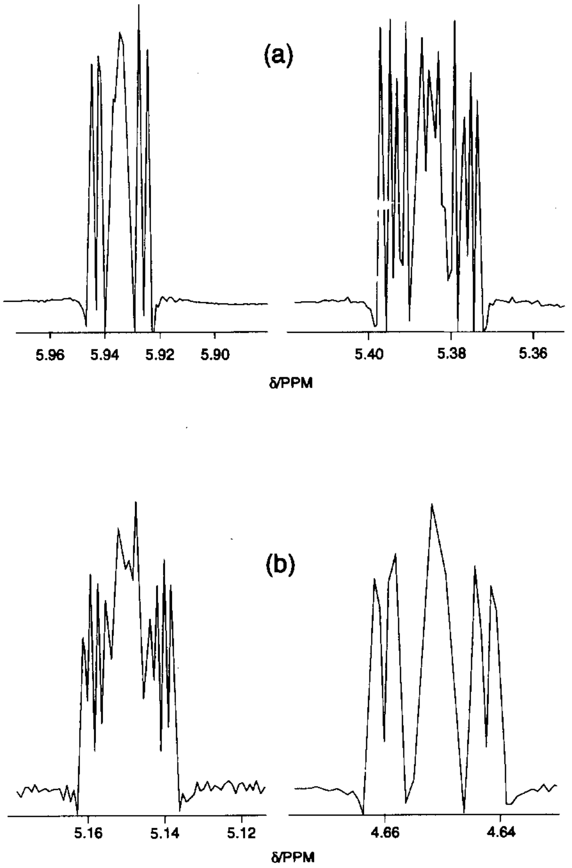

Fig. 4. ^{1}H NMR resonances of the Cp nuclei in (a) **I** and (b) **III**.

3.2. Hydrogen-1 NMR spectra

Table 5 gives the ^{1}H NMR assignments for **I** and related compounds according to the numbering scheme shown in Fig. 3. The relative ordering of the resonances for the H(1), H(4) and H(2), H(3) Cp ring atom pairs in **I**, **IV**, **V** and **VI** is that expected on the basis of diamagnetic anisotropic effects. In addition, differences between $^{103}Rh-^{1}H$ Cp coupling constants (0.1–0.2 Hz) are smaller for these compounds than for **III** and **VII**. The ordering of these resonances is also reversed at ambient temperature (Fig. 4) in the case of **III**. We interpret this pattern as indicative of a higher allyl-ene rotamer population in **III**. A definitive assignment of the signals from the ring hydrogen nuclei in **VI** and **VII** was obtained from nOe difference experiments [17]. These studies also permitted identification of the conformational preference of the ring relative to the counter diene ligand [18]. In both cases (Fig. 5) these orientations are remarkably similar to those determined from crystallographic studies of closely related compounds [16]. On cooling a sample of **VII** from 294 to 213 K, the resonances assigned to H(2) and H(3)

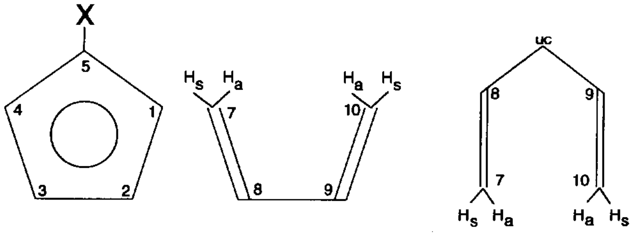

Fig. 3. The atom-numbering system for Tables 5–7.

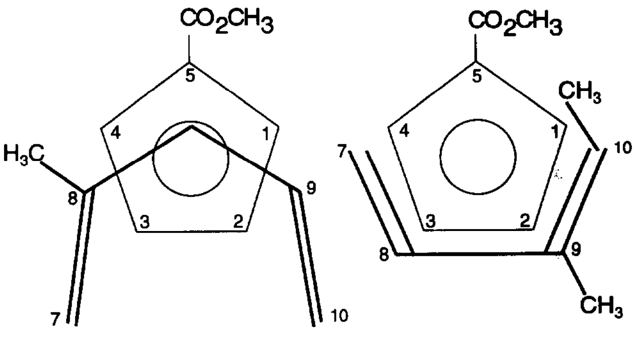

Fig. 5. The orientation of ligands in solution for **VI** and **VII** as determined from nOe difference spectra.

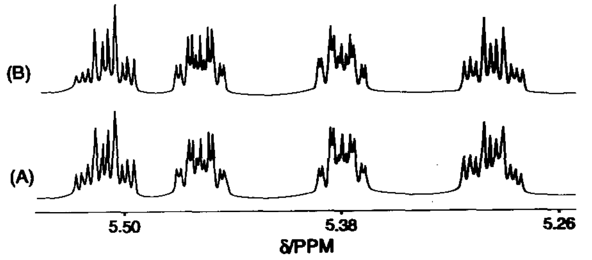

Fig. 6. Experimental (curve (A)) and simulated (curve (B)) 250 MHz ^1H NMR spectrum of the ring nuclei of **VII**.

move to a lower field while those of H(1) and H(4) move to a higher field. Coville and coworkers [19] have reported similar effects in variable-temperature NMR spectra of [η^5-$C_9H_7Ru(CO)(PPh_3)$ (I)] but, unlike that for **VII**, the resonance half-width of the ring signals is also temperature dependent and signal convergence and cross-over (Table 5) is not observed. The behaviour of the ruthenium complex has been associated with hindered rotation, although it was also suggested that the effect could be a manifestation of ring slippage. The behaviour of **VII** is in accord with an increasing population of the allyl-ene rotamer as the temperature is decreased. A simulation study was performed on the ring nuclei of **VI** and **VII** by use of the PANIC program [17]. Figure 6 shows the experimental and simulated spectra for **VII**, and Table 6 gives the coupling constant data for **VI** and **VII**. It is noteworthy that these values differ appreciably from those determined for monosubstituted ferrocenes [20] and ferroceneophanes [21]; the difference probably reflects the sensitivity of the ring to electronic perturbation. The better π acceptor properties of the 2,3-dimethoxybutadiene ligand are reflected in the remarkable chemical shift ($\delta = -0.27$ ppm) for the terminal antihydrogen nuclei in **II** and the larger coupling constants from rhodium to H(7_s) and H(7_a) for **I** and **II** compared with those found for **III**, **IV** or **V**. No metal-diene-hydrogen coupling could be detected in the case of **VII**.

3.3. Carbon-13 NMR spectra

^{13}C NMR data for **I–VII** are presented in Table 7. HETCOR techniques were employed in the assignment of resonances. The respective average values for terminal and internal C–H one-bond coupling for the diene in **I** and **IV** are 159.6 Hz, 160.0 Hz and 168.0 Hz, values very similar to those observed for (η^4-butadiene)$Fe(CO)_3$ [22]. Although the values of these couplings have been commonly used as a guide to changes in hybridization of coordinated olefin carbons, their true value is open to question. This is because of the presence of substituents and changes in the geometry of the coordinated ligand [23], which will also affect the size of the coupling constants. For example the metal, as an electropositive substituent, would be expected to cause some reduction in C–H coupling at the diene terminus [24]. Since the olefin C–H one-bond coupling is 161 Hz for cyclopentene, an appreciable bonding contribution from a metallocyclopentene form would not be expected to be accompanied by significant changes in one-bond C–H coupling for the internal diene carbon atoms. A similar ambiguity exists for unconjugated diene and ethene systems, for which no pronounced changes in ^1J(C–H) would be expected between the extremes of metallocyclopropane or η^2-olefin bonding [25]. In view of these problems we regard the metal–carbon couplings as a more reliable indicator of the type of metal–ligand bonding. As a consequence of the small magnetogyric ratio of ^{103}Rh all observed rhodium–carbon couplings fall within a relatively small range, and it has been suggested that the magnitude reflects the s character of the metal–carbon bond [26]. In [(η^2-$C_2H_4)_2RhC_5H_4X$] compounds the olefin–metal coupling is 13.2 Hz [27]. The corresponding value for non-conjugated diene compounds such as **VII** varies from 13.2 to 15.1 Hz and is always smaller than that observed (16.5–17.6 Hz) for butadiene analogues [11] for **III** and **IV**, which show intermediate values of 14.5 Hz and 14.8 Hz respectively. This is consistent with the bonding characteristics of *trans,trans*-1,4-diphenylbutadiene. Jolly and Mynott [28] have defined a parameter ρ as the ratio $\Delta\delta(C(7))/\Delta\delta(C(8))$ of coordination chemical shifts of terminal and internal carbon atoms of the coordinated 1,3-diene in a variety of metal-(η^4-butadiene) complexes. They observed that compounds with larger ρ and smaller $\Delta\delta(C(8))$ values are also those in which metal–diene back bonding is more important. The ρ values for the diene ligand in **I**, **V** and **III** are 1.96, 1.54

TABLE 6. Cyclopentadienyl ring hydrogen coupling constants for **VI** and **VII**

Compound	Coupling constants (±0.02 Hz)									
	J_{12}	J_{23}	J_{34}	J_{13}	J_{14}	J_{24}	J_{Rh-1}	J_{Rh-2}	J_{Rh-3}	$J_{Rh-H(4)}$
VI	1.54	2.70	1.64	2.77	1.56	2.76	0.83	1.10	0.95	0.79
VII	1.67	2.74	1.66	2.75	1.63	2.75	0.50	0.92	0.99	0.51

TABLE 7. Carbon-13 nuclear magnetic resonance spectral data for $[\eta^5C_5H_4X)Rh(diolefin)$ with ^{103}Rh coupling constants in parentheses [a]

Compound	Diolefin	^{13}C NMR, δ (ppm)											
		X	C(5)	C(1)	C(4)	C(2)	C(3)	X	C(7)	C(10)	C(8)	C(9)	Me
I	2,3-Dimethoxy-butadiene	CHO	99.13 (J = 5.8 Hz)	84.99 (J = 4.5 Hz)		87.42 (J = 4.5 Hz)		185.10	19.01 (J = 17.1 Hz) [63.70] [b]		124.50 (J = 5.7 Hz) [32.40] [b]		56.05
II	2,3-Dimethoxy-butadiene	H	83.10 (J = 5.0 Hz)						16.5 (J = 17.4 Hz)		123.41 (J = 5.9 Hz)		56.70
III	*trans,trans*-1,4-Diphenylbutadiene	CHO	99.36 (J = 6.0 Hz)	89.93 (J = 4.8 Hz)		90.10 (J = 5.8 Hz)		185.57	58.05 (J = 14.5 Hz) [71.27] [b]		78.39 (J = 8.0 Hz) [54.41] [b]		133.34 (Ph)
IV	*trans,trans*-1,4-Diphenylbutadiene	COOMe	91.65 (J = 5.8 Hz)	89.22 (J = 5.3 Hz)		89.00 (J = 5.3 Hz)		166.40 (J = 52.0 Hz)	57.23 (J = 14.8 Hz)		77.92 (J = 8.0 Hz)		131.60 (Ph)
V	2,3-Dimethyl-butadiene	CHO	99.36 (J = 5.4 Hz)	84.55 (J = 4.9 Hz)		88.54 (J = 5.3 Hz)		185.0	38.79 (J = 16.5 Hz) [74.36] [b]		94.91 (J = 7.8 Hz) [48.4] [b]		20.02
VI	*cis*-3-Methyl-pentadiene	COOMe	90.70 (J = 5.3 Hz)	86.82 (J = 4.2 Hz)	86.65 (J = 5.0 Hz)	87.88 (J = 4.4 Hz)	86.66 (J = 4.9 Hz)	168.88 (J = 51.95 Hz)	35.94 (J = 17.8 Hz)	48.21 (J = 17.7 Hz)	84.74 (J = 6.9 Hz)	95.50 (J = 5.3 Hz)	15.80 (J = 4.0 Hz) [24.37] [b]
VII	2-Methyl-1,4-pentadiene [c]	COOMe	93.04 (J = 4.7 Hz)	86.33 (J = 4.3 Hz)	86.96 (J = 3.9 Hz)	89.19 (J = 3.9 Hz)	89.13 (J = 3.8 Hz)	165.76 (J = 51.22 Hz)	43.69 (J = 15.1 Hz)	43.34 (J = 14.9 Hz)	45.28 (J = 8.6 Hz)	26.19 (J = 8.6 Hz)	29.32 (J = 1.7 Hz)

[a] Recorded in $CDCl_3$ at 294K relative to internal $SiMe_4$.

[b] Diene coordination shifts in square brackets.

[c] Chemical shift δ of uncoordinated diene carbon is 35.95 ppm with through-space coupling to rhodium of 2.86 Hz.

and 1.31. This trend reflects the diminishing importance of metal–diene retrodative bonding, although the values of the coordination shift for C(8) indicates that in all cases the butadiene moiety is acting as an η^4 ligand. The rhodium–Cp couplings range from 3.8 to 6.0 Hz in the compounds listed in Table 7. The coupling to the nodal carbon C(5) is usually largest and, of the atom pair C(1) and C(4) and the atom pair C(2) and C(3), it is the latter that commonly shows the larger metal coupling. Since rhodium–π allyl carbon coupling ranges from 4 to 12 Hz, compared with from 6 to 17 Hz for rhodium–olefin coupling [29], the relative ordering of the Cp–metal couplings is in the correct sense, although it is accepted that the dominant bonding mode is primarily delocalized in these systems.

Acknowledgments

We thank Glaxo Group Research (Ware) for a generous gift of rhodium trichloride and Dr. O. Howarth for the nOe difference spectra.

References

1 M. Arthurs, C. Piper, D.A. Morton-Blake and M.G.B. Drew, *J. Organomet. Chem., 429* (1992) 257
2 H.G. Schuster-Woldan and F. Basolo, *J. Am. Chem. Soc., 88* (1966) 1657.
3 M. Cheong and F. Basolo, *Organometallics, 7* (1988) 2041.
4 D.L. Lichtenberger, D.C. Calabro and G.E. Kellogg, *Organometallics, 3* (1984) 1623.
5 D. Rehder, *Coord. Chem. Rev., 110* (1991) 161.
6 Y. Wakatsuki, H. Yamazaki, T. Kobayashi and Y. Sugawara, *Organometallics, 6* (1987) 1191.
7 R. Benn, K. Cibura, P. Hofmann, K. Jonas and A. Rufinska, *Organometallics, 4* (1985) 2214.
8 M. Arthurs, S.M. Nelson and M.G.B. Drew, *J. Chem. Soc., Dalton Trans.*, (1977) 779.
9 R. Cramer and L.P. Seiwell, *J. Organomet. Chem., 92* (1975) 245.
10 A.L. van Geet, *Anal. Chem., 42* (1970) 679.
11 M. Arthurs, E. Curzon, P. Gross, G. Kubal, L. Paniwnyk and C. Piper, *J. Organomet. Chem., 366* (1989) 223.
12 D.L. Lichtenberger, C.H. Blevins and R.B. Ortega, *Organometallics, 3* (1984) 1614.
13 M.G.B. Drew, S.M. Nelson and M. Sloan, *J. Organomet. Chem., 39* (1972) C9.
14 A. Baba-Ahmed and J. Gayoso, *Theor. Chim. Acta, 62* (1983) 507; A. Baba-Ahmed, J. Gayoso, B. Maouche and O. Oumerali, *Rep. QCPE 474*, 1983, Indiana University.
15 N. Sakai, K. Mashima, H. Takaya, R. Yamaguchi and S. Kozima, *J. Organomet. Chem., 419* (1991) 181.
16 M. Arthurs, H. Karodia, M. Sedgwick, D.A. Morton-Blake, C.J. Cardin and H. Parge, *J. Organomet. Chem., 291* (1985) 231.
17 P. Johnston, M.S. Loonat, W.L. Ingham, L. Carlton and N.J. Coville, *Organometallics, 6* (1987) 2121.
18 J. du Toit, D.C. Levendis, J.C.A. Boeyens, M.S. Loonat, L. Carlton, W. Pickl and N.J. Coville, *J. Organomet. Chem., 368* (1989) 72.
19 M.S. Loonat, L. Carlton and N.J. Coville, *S. Afr. J. Chem., 41* (1988) 72.
20 N. Kamezawa, *J. Magn. Reson., 11* (1973) 88.
21 R.R. McGuire, R.E. Cochoy and J. Winstead, *J. Organomet. Chem., 84* (1975) 269.
22 K. Bachmann and W. von Philipsborn, *Helv. Chim. Acta, 63* (1980) 773.
23 H. Friebolin, *Basic One and Two-dimensional NMR Spectroscopy*, VCH, Weinheim, 1991, p. 85.
24 H. Gunther, *NMR Spectroscopy - An Introduction*, Wiley, Chichester, West Sussex, 1987, p. 375.
25 C.A. Tolman, A.D. English and L.E. Manzer, *Inorg. Chem., 14* (1975) 2353.
26 C. Elschenbroich and A. Salzer, *Organometallics, A Concise Introduction*, VCH, Weinheim, 1989, p. 301.
27 M. Arthurs, H.K. Al-Daffaee, J. Haslop, G. Kubal, M.D. Pearson, P. Thatcher and E. Curzon, *J. Chem. Soc., Dalton Trans.*, (1987) 2615.
28 P.W. Jolly and R. Mynott, *Adv. Organomet. Chem., 19* (1981) 257.
29 P. Powell and L.J. Russell, *J. Organomet. Chem., 129* (1977) 415.